Angle-Resolved Photoemission Spectroscopy of Tetragonal CuO: Evidence for Intralayer Coupling Between Cupratelike Sublattices

S. Moser,[1,2] L. Moreschini,[2] H.-Y. Yang,[3] D. Innocenti,[2,4] F. Fuchs,[5] N. H. Hansen,[5,6] Y. J. Chang,[2,7] K. S. Kim,[2,9,10] A. L. Walter,[2,8] A. Bostwick,[2] E. Rotenberg,[2] F. Mila,[3] and M. Grioni[1]

[1]*Institute of Condensed Matter Physics, Ecole Polytechnique Fédérale de Lausanne (EPFL), CH-1015 Lausanne, Switzerland*
[2]*Advanced Light Source (ALS), Berkeley, California 94720, USA*
[3]*Institute of Theoretical Physics, Ecole Polytechnique Fédérale de Lausanne (EPFL), CH-1015 Lausanne, Switzerland*
[4]*Dipartimento di Ingegneria Meccanica, Università di Roma Tor Vergata, I-00133 Roma, Italy*
[5]*Experimental Physics VI, Julius-Maximilian University of Würzburg, 97074 Würzburg, Germany*
[6]*ZAE Bayern, Am Hubland, 97074 Würzburg, Germany*
[7]*Department of Physics, University of Seoul, Seoul 130-743, Korea*
[8]*Department of Physical Chemistry, Fritz-Haber-Institut der Max-Planck-Gesellschaft, Faradayweg 4-6, D-14195 Berlin, Germany*
[9]*Department of Physics, Pohang University of Science and Technology, Pohang 790-784, Korea*
[10]*Center for Artificial Low Dimensional Electronic Systems, Institute for Basic Science, Pohang 790-784, Korea*

(Received 11 April 2014; published 30 October 2014)

We investigate by angle-resolved photoemission the electronic structure of *in situ* grown tetragonal CuO, a synthetic quasi-two-dimensional edge-sharing cuprate. We show that, in spite of the very different nature of the copper oxide layers, with twice as many Cu in the CuO layers of tetragonal CuO as compared to the CuO_2 layers of the high-T_c cuprates, the low-energy electronic excitations are surprisingly similar, with a Zhang-Rice singlet dispersing on weakly coupled cupratelike sublattices. This system should thus be considered as a member of the high-T_c cuprate family, with, however, interesting differences due to the intralayer coupling between the cupratelike sublattices.

DOI: 10.1103/PhysRevLett.113.187001 PACS numbers: 74.25.Jb, 74.20.Pq, 74.72.Cj

The physics of cuprates is remarkably rich, ranging from high-temperature superconductors (HTSs) [1,2] to spin ladders [3,4]. Their properties derive from the structure of the copper oxide layers, which evolves from CuO_2 in HTSs to Cu_2O_3 in spin ladders by fitting more and more coppers into the layers, as in the family $Sr_{n-1}Cu_{n+1}O_{2n}$ ($n = 3, 5, \ldots$) [5]. Synthesizing systems with pure two-dimensional (2D) CuO layers would be fascinating, but this goal has remained elusive. Interestingly, CuO—which has been studied as a model parent compound for the HTS cuprates due to its simple stoichiometry [6,7]—does not contain copper oxide layers. Its low-symmetry monoclinic tenorite structure consists of crossed ribbons of edge-sharing CuO_4 plaquettes [8], and its magnetic excitations have 1D character (spinons) [9,10].

A tetragonal (elongated rocksalt) structure, much closer to that of the HTS cuprates, can be stabilized up to a thickness of several unit cells [11,12] when CuO is grown epitaxially on a $SrTiO_3$ (001) substrate [13]. In tetragonal CuO (T-CuO), the Cu ions are at the center of edge-sharing elongated CuO_6 octahedra, which form infinite CuO planes stacked along the c axis. The ratio of the apical- to in-plane Cu-O distances is large (1.37), which reduces the interplane coupling. The inset of Fig. 1(a) illustrates the structure of a CuO plane, paved by edge-sharing CuO_4 plaquettes. The red square, which outlines one plaquette, is also the 2D unit cell, and a is the side of the 3D tetragonal unit cell. In this structure, copper atoms form a square lattice, but the oxygens are *not* between nearest neighbor (NN) coppers, as in the CuO_2 layers of the cuprates, but between next-NNs. As a consequence, the hopping and exchange parameters are expected to be quite small between NN coppers. Indeed, the $Sr_{n-1}Cu_{n+1}O_{2n}$ family consists of essentially decoupled spin ladders because the exchange coupling between NNs located in edge-sharing CuO_4 plaquettes is very small [3,4]. To which extent the electronic properties of the CuO layers are related to those of the CuO_2 layers of the cuprate parent compounds is one of the important questions addressed by the present work. Some basic information about the electronic structure of T-CuO has been obtained by first-principles density functional [14,15] and by LDA + U calculations [16], but the band structure has not been discussed or measured yet. The interest in this new material also stems from its predicted magnetic properties. An extrapolation from the behavior of other 3d transition metal monoxides, from MnO to NiO, suggests that the Néel temperature T_N of T-CuO could be as high as 700–800 K [11]. A very recent experiment finds $T_N = 600$ K [17]. Such enhanced antiferromagnetic (AFM) coupling would open the way to new practical applications, but would also be quite interesting for scenarios of HTSs based on magnetic fluctuations [18].

Figure 1 gives an overview of the ARPES results on a thin film (6 unit cells) T-CuO sample. Figure 1(a) is a composite k_x vs k_y ARPES constant energy map measured at the top of the valence band E_V. The ARPES features in

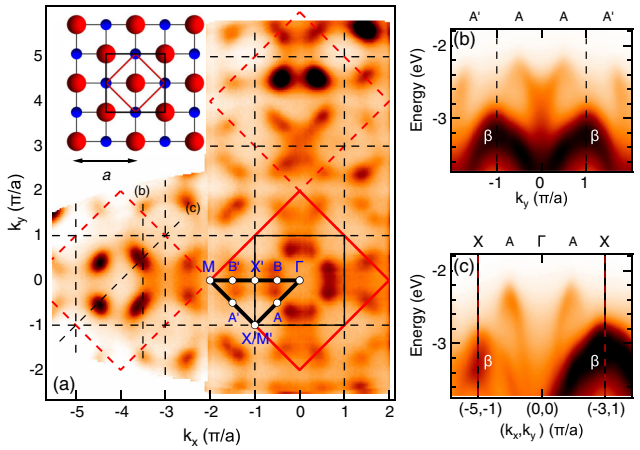

FIG. 1 (color online). (a) Constant energy map at E_V, measured at $h\nu = 120.5$ eV and $T = 90$ K. It is a composite of two data sets, one centered at $k_x = -4\pi/a$, the other at $k_x = 0$ ($\overline{\Gamma M} = 2\pi/a = 1.61$ Å^{-1}, $\overline{\Gamma X} = \sqrt{2}\pi/a = 1.14$ Å^{-1}). The red and black squares are the BZs corresponding to the unit cells defined in the inset. (inset) The structure of a CuO plane: Cu (O) ions are indicated in red (blue). The red square is the 2D unit cell, which coincides with a CuO_4 plaquette; "a" is the length of the side of the 3D tetragonal unit cell. The black square is the nonprimitive $c(2 \times 2)$ unit cell. (b) and (c) show the E vs k dispersion along lines (b) and (c) in panel (a).

an energy window of at least 1 eV below E_V do not disperse as a function of the perpendicular wave vector k_z [13]; i.e., they have nearly 2D character. The map shows four strong intensity maxima, offset by 90°, in the first Brillouin zone (BZ), outlined by the red square in Fig. 1(a), corresponding to the crystallographic surface unit cell. The fourfold pattern can be recognized in all adjacent BZs, outlined by dashed red squares, even if intensities are modulated by ARPES matrix elements. Namely, the signal is suppressed along the lines $k_x = \pm k_y$, crossing at (0,0), reflecting the scattering geometry and the symmetry of the Cu $d_{x^2-y^2}$ orbitals [13]. A closer inspection, however, reveals weaker replicas of this pattern in both the k_x and k_y directions, leading to an overall periodicity which is that of a two times smaller Wigner-Seitz cell in reciprocal space, rotated by 45° and shown in black. It is the BZ of a $c(2 \times 2)$ unit cell (shown in black in the inset) containing two Cu ions. It would be the relevant BZ if the layer were divided into two noninteracting sublattices, since it would correspond to the primitive unit cell of each sublattice. This is the first experimental indication that the coupling between the two sublattices through the interaction between NN copper atoms must be small.

The band dispersion is illustrated in Figs. 1(b) and 1(c). To avoid complications due to the intensity suppression along the diagonals $k_x = \pm k_y$, here and in the following we will discuss data collected from the BZ centered at $(-4\pi, 0)$. In addition to the usual Γ, X, and M points, it will prove useful to define the midpoint X' between Γ and M (the X point of the small BZ), and pairs of points A, A', and B, B', symmetric with respect to the XX' line. If the two sublattices were completely decoupled, the pairs of points (Γ, M), (A, A') and (B, B') would be equivalent. Figures 1(b) and 1(c) present two E vs $k_{\|}$ cuts along the lines marked (b) and (c) in Fig. 1(a). Cut (b) shows a band with maxima at $E = -2.35$ eV at the A points of the BZ, in correspondence of the intensity maxima of Fig. 1(a). This sets a lower limit to the band gap of T-CuO, which is therefore larger than in bulk CuO (1.35 eV [19]). The secondary maxima at $E = -2.5$ eV at the A' points, coincide with the replica features. The dispersion outlines the momentum dependence of the first ionization state of an edge-sharing CuO plane. As further discussed below, this is the Zhang-Rice singlet (ZRS) band [20], typical of the 2D corner-sharing cuprates, i.e., a band with $^1A_1$ symmetry, mainly $d^9\underline{L}$ character, with both holes in wave functions with b_{1g} symmetry (one in the $d_{x^2-y^2}$ orbital of Cu, the other one in an appropriate linear combination of p orbitals of neighboring oxygens). It merges around -3 eV with a more intense band (labeled β) with a maximum at the X point. By analogy with the 2D corner-sharing cuprates, we assign the latter to a manifold of $d^9\underline{L}$ states of different orbital symmetries [7].

Figure 2(a) illustrates the experimental band structure measured along a $\Gamma MX\Gamma$ contour, equivalent to the triangular contour of Fig. 1(a), in the BZ centered at $(-4\pi, 0)$. For the ZRS band, blue circles outline the

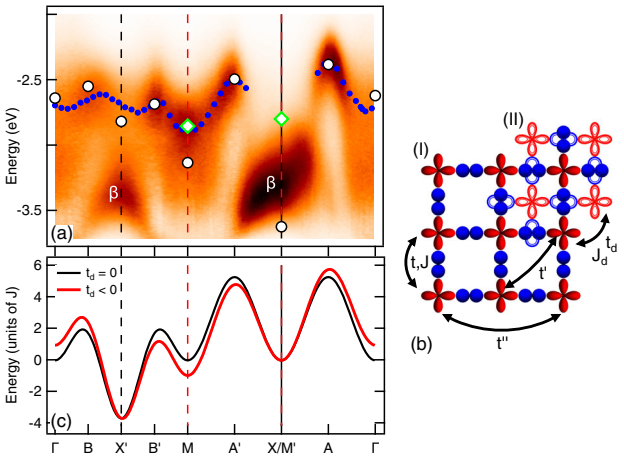

FIG. 2 (color online). (a) ARPES dispersion along a triangular contour equivalent to that of Fig. 1(a), in the BZ centered at $(-4\pi, 0)$. The data have been normalized to the same integrated intensity for all k values, after subtraction of an integral (Shirley) background. Filled (blue) symbols outline the experimental dispersion of the ZRS band. Empty circles (diamonds) mark the peak positions calculated by an extended t-J model, whose parameters are defined in panel (b). The CuO plane is seen as the superposition of two corner-sharing sublattices (I) and (II). (c) Dispersion of the lower Hubbard band from Ref. [21] (black line), and illustration of the degeneracy lifting induced by a finite hopping $t_d = -0.03$ eV between the two sublattices.

dispersion of the ARPES peak. Along the $A'XA$ path the broad line shape (see below) prevents a reliable determination of the peak position. The emergent symmetry suggested by the intensity map is still partially reflected in these data, but not fully since the pairs (Γ, M), (A, A'), and (B, B') are not strictly equivalent. As a first step to interpret the experimental data, we have plotted in Fig. 2(c) the dispersion for the lower Hubbard band:

$$E(k) = -4t'[\cos(k_x a)\cos(k_y a)] - 2t''[\cos(2k_x a) + \cos(2k_y a)] - J[\cos(k_x a) + \cos(k_y a)]^2,$$

with $t' = -0.12$ eV, $t'' = 0.08$ eV and $J = 0.125$ eV used to fit the ARPES data for a single hole in the AFM background of the corner-sharing insulating cuprate Ca_2CuOCl_2 [21]. This dispersion should be a good starting point if the CuO plane is seen as the superposition of the two interpenetrating corner-sharing sublattices (I) and (II) of Fig. 2(b), as long as they are weakly coupled. It qualitatively captures the main features of the experimental dispersion, namely, the location of the band maxima and minima, but of course cannot quantitatively reproduce the energy difference between the pairs (A, A'), (B, B'), and (Γ, M). Adding a "diagonal" hopping t_d between the two lattices, the dispersion becomes

$$E'(k) = E(k) - 4t_d[\cos(k_x a/2)\cos(k_y a/2)],$$

which yields the red line in Fig. 2(c). The symmetry of the original lattice, corresponding to the larger (red) BZ in Fig. 1(a), is qualitatively recovered. The A, A', B, B', and Γ, M pairs of points are no longer equivalent, and the degeneracies are lifted, in qualitative agreement with the experiment, where $E(\Gamma) - E(M) = 180$ meV, $E(A) - E(A') = 140$ meV and $E(B) - E(B') = 60$ meV.

The model of Fig. 2(c), which consists in just adding a diagonal hopping to the dispersion of the excitations on the underlying sublattices, has mainly a pedagogical value, and cannot fully describe the complex dynamics of a strongly correlated hole propagating in the AFM background of the edge-sharing CuO plane. As a further step, we consider a generalized t-J model [22,23]:

$$\tilde{H}_{tJ} = J\sum_{i,j}\vec{S}_i\cdot\vec{S}_j - t\sum_{i,j,\sigma}\hat{c}^\dagger_{i,\sigma}\hat{c}_{j,\sigma} - t'\sum_{i,j',\sigma}\hat{c}^\dagger_{i,\sigma}\hat{c}_{j',\sigma} - t''\sum_{i,j'',\sigma}\hat{c}^\dagger_{i,\sigma}\hat{c}_{j'',\sigma} + J_d\sum_{i,m}\vec{S}_i\cdot\vec{S}_m - t_d\sum_{i,m,\sigma}\hat{c}^\dagger_{i,\sigma}\hat{c}_{m,\sigma}.$$

Unprimed, primed, and double-primed indices refer to first, second, and third NNs on the same sublattice; m indicates NNs on the whole lattice.

Since the local geometry of the corresponding bonds is very similar to that of cuprates, we have adopted for t, t', t'', and J typical values for cuprate superconductors taken from Ref. [24]. The diagonal hopping and exchange terms have been determined from a Cu_2O_6 cluster along the lines of Ref. [25]. The coupling terms t_d and J_d reflect the $Cu(I)d_{x^2-y^2} - O(I)p_{x,y} - O(II)p_{x,y} - Cu(II)d_{x^2-y^2}$ orbitals' overlap. We found a small but non-negligible $t_d \sim -t/4 = -100$ meV and a very weak AFM exchange: $J_d = 6$ meV. We then performed an exact diagonalization of $\tilde{H}_{tJ}$ on a 32-site cluster to calculate the hole spectral function $A(\vec{k}, \hbar\omega)$ (Fig. 3, right column). For our 32-site cluster, $A(\vec{k}, \hbar\omega)$ is only defined at a small number of k points. The corresponding spectra are shown in the left column of Fig. 3, normalized to the same total integrated intensity. For each k point, the lowest-energy peak represents the coherent spectral weight. Those at higher energies belong to the incoherent spectral weight, which reflects dressing by electronic and magnetic excitations. The incoherent weight varies strongly from point to point. It is never small, and even becomes dominant at the M and X points, reflecting strong and k-dependent correlations. To enable a comparison with the ARPES spectra shown in the left column, a 500 meV Gaussian broadening was applied to the calculated spectra. This is much larger than the experimental energy resolution (30 meV), but typical of ARPES data from insulating cuprates [21]. The peak energies of the broadened spectra are shown as empty circles in Fig. 2(a). For the M and X points, the peak energies are clearly not representative of the energy of the excitations, which are then separately indicated by empty diamonds. The theory describes the overall ZRS dispersion very well, and captures the inequivalence of the pairs of points (A, A'), (B, B'), and (Γ, M). The finite size of the cluster leads to a discretization and an underestimation of the incoherent

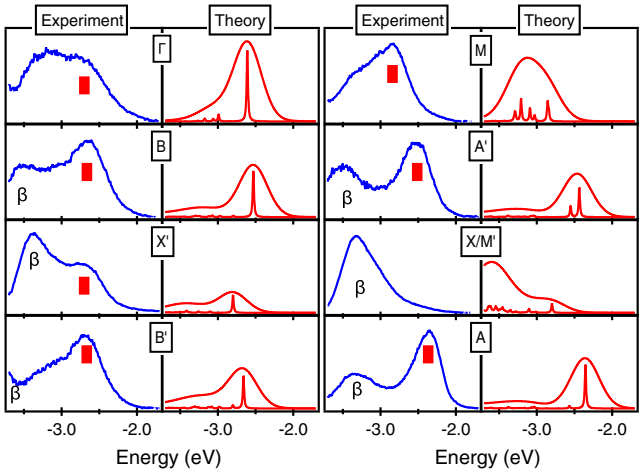

FIG. 3 (color online). Comparison of the ARPES spectra extracted from Fig. 2(a) with the calculated spectral function of our cluster model with and without a 500 meV broadening. Red tags mark the position of a prominent ARPES dispersing feature [blue circles in Fig. 2(a)] and do not always coincide with the energy of the excitations.

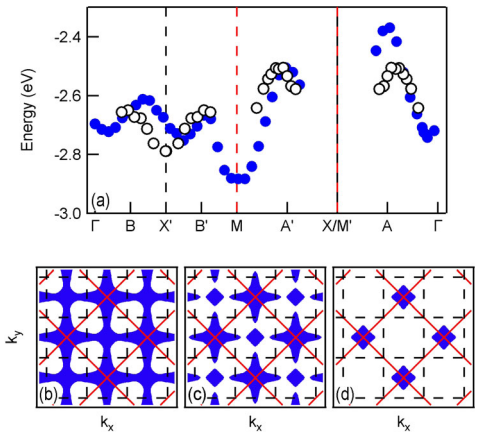

FIG. 4 (color online). (a) The experimental dispersion of the first ionization state in T-CuO (full symbols) is compared with that of the ZRS band in $Sr_2CuO_2Cl_2$ (empty symbols) [26], along the same triangular contour as in Fig. 2. (Bottom) Calculated Fermi surface of T-CuO for various hole dopings n: (b) $n = 0.07$; (c) $n = 0.37$; (d) $n = 0.80$ holes/Cu ion. Details of the calculations are in Ref. [13].

spectral weight. Nevertheless, the experimental spectra are well reproduced, namely, the double peak structures at Γ and M, and especially the suppression of the coherent spectral weight around X. Let us emphasize that, on the basis of the present data and calculation, a determination through fitting of all hopping parameters is not possible. This is why we have adopted parameters typical of cuprates for t, t', t''. However, the experimental results seriously constrain the value of the intralayer coupling t_d between the sublattices. In particular, the splitting between the peaks at A and A' is proportional to t_d with a coefficient that depends only weakly on the other parameters, and the experimental splitting of 140 meV imposes a value of $t_d \sim -100$ meV to a good accuracy.

We can now compare the electronic structure of edge-sharing T-CuO with that of a representative corner-sharing cuprate. Figure 4(a) shows the first ionization state of T-CuO, and the ZRS band of $Sr_2CuO_2Cl_2$ [26]. The energies of the two bands have been aligned at the A' point maximum. The two dispersions are quite similar, notwithstanding the already discussed asymmetry of the conjugated points in T-CuO. This conclusively supports the assignment of the topmost band in CuO to the ZRS. The observation of a sharp kink in the momentum-dependent spectral weight distribution [13] reinforces the similarity with the electronic structure of the HTS parent compounds.

Our ARPES data indicate that the CuO layers of T-CuO are best understood as weakly coupled cupratelike sublattices. Accordingly, the electronic and magnetic properties can be expected to be very similar. However, as we will now briefly discuss, the weak coupling between the cupratelike sublattices can induce qualitative differences for some properties. At half filling, which is the case of the samples available so far, the system is a charge-transfer insulator, and in the limit of an infinite stack, it is expected to develop AFM order, with potentially a very high Néel temperature due to the stronger interlayer coupling than in high-T_c cuprates, an expectation very recently confirmed [17]. This is not the whole story, however. Since each layer consists of two weakly coupled copies of the AF Heisenberg model on a square lattice, the ordering can take place with wave vector $(0, \pi)$ or $(\pi, 0)$ in the plane, leading to an additional Ising order parameter [27–29]. According to a recent study [30], there are two scenarios for the phase transition. If the interlayer coupling is large the system will undergo a *first-order* transition to a low-temperature phase where both the Ising and the Néel order parameter acquire a finite value, while for small interlayer coupling there should be a sequence of two phase transitions first to a phase with Ising order [fluctuations choose between $(0, \pi)$ or $(\pi, 0)$], then to a phase with 3D AFM order. Although the results of Ref. [17] point to a single transition, further experimental investigations of the ordering process are necessary to fully clarify its nature.

Doping T-CuO away from half filling cannot be achieved chemically without introducing disorder in the CuO layers, but it may be realized in principle by a field effect approach employing ionic liquids [31]. This is a real challenge, and we will only briefly discuss this possibility here. By analogy to, e.g., Na-doped $Ca_2CuO_2Cl_2$ [32,33], the system can be expected to develop superconductivity upon doping. The two-sublattice structure has an interesting consequence, however. As shown in Fig. 4, when the Fermi surface changes from holelike to electronlike, two types of electron pockets with different numbers of carriers would appear before another change of topology takes place that leads to a single type of electron pocket. This should be contrasted to the case of the high-T_c cuprates where there is always only one type of pocket for both the electron and hole Fermi surface. The consequences on superconductivity are left for future investigation.

We acknowledge support by the Swiss NSF, in particular through Grant No. PA00P21-36420 (L. M.). We thank C. Proust, B. Vignolle, J. Denlinger, A. Damascelli, S. Nemsak, and C. Tournier-Colletta for valuable discussions. The Advanced Light Source is supported by the Director, Office of Science, Office of Basic Energy Sciences, of the U.S. Department of Energy under Contract No. DE-AC02-05CH11231. S. M. and L. M. contributed equally to this work.

[1] J. G. Bednorz and K. A. Müller, Z. Phys. B **64**, 189 (1986).
[2] M. K. Wu, J. R. Ashburn, C. J. Torng, P. H. Hor, R. L. Meng, L. Gao, Z. J. Huang, Y. Q. Wang, and C. W. Chu, Phys. Rev. Lett. **58**, 908 (1987).
[3] E. Dagotto and T. M. Rice, Science **271**, 618 (1996).

[4] M. Azuma, Z. Hiroi, M. Takano, K. Ishida, and Y. Kitaoka, Phys. Rev. Lett. **73**, 3463 (1994).
[5] Z. Hiroi, M. Azuma, M. Takano, and Y. Bando, J. Solid State Chem. **95**, 230 (1991).
[6] J. Zaanen, G. A. Sawatzky, and J. W. Allen, Phys. Rev. Lett. **55**, 418 (1985).
[7] H. Eskes, L. H. Tjeng, and G. A. Sawatzky, Phys. Rev. B **41**, 288 (1990).
[8] S. Åsbrink and L. J. Norrby, Acta Crystallogr. Sect. B **26**, 8 (1970).
[9] A. T. Boothroyd, A. Mukherjee, S. Fulton, T. G. Perring, R. S. Eccleston, H. A. Mook, and B. M. Wanklyn, Physica (Amsterdam) **234B**, 731 (1997).
[10] S.-H. Jung, J. Kim, E. J. Choi, Y. Sekio, T. Kimura, and J. Lorenzana, Phys. Rev. B **80**, 140516(R) (2009).
[11] W. Siemons, G. Koster, D. H. A. Blank, R. H. Hammond, T. H. Geballe, and M. R. Beasley, Phys. Rev. B **79**, 195122 (2009).
[12] D. Samal, H. Tan, Y. Takamura, W. Siemons, J. Verbeeck, G. Van Tendeloo, E. Arenholz, C. A. Jenkins, G. Rijnders, and G. Koster, Europhys. Lett. **105**, 17 003 (2014).
[13] See Supplemental Material at http://link.aps.org/supplemental/10.1103/PhysRevLett.113.187001 for sample growth, supplementary ARPES data, a discussion of ARPES intensities, and details on the model.
[14] G. Peralta, D. Puggioni, A. Filippetti, and V. Fiorentini, Phys. Rev. B **80**, 140408(R) (2009).
[15] X.-Q. Chen, C. L. Fu, C. Franchini, and R. Podloucky, Phys. Rev. B **80**, 094527 (2009).
[16] P. M. Grant, J. Phys. Conf. Ser. **129**, 012042 (2008).
[17] K. S. Rabinovich, L. L. Samollenko, A. S. Zhuravleva, and A. G. Shneider, Appl. Phys. Lett. **104**, 182406 (2014).
[18] A. Abanov, A. Chubukov, and A. V. Schmalian, Adv. Phys. **52**, 119 (2003).
[19] F. P. Koffyberg and F. A. Benko, J. Appl. Phys. **53**, 1173 (1982).
[20] F. C. Zhang and T. M. Rice, Phys. Rev. B **37**, 3759 (1988).
[21] F. Ronning, C. Kim, D. L. Feng, D. S. Marshall, A. G. Loeser, L. L. Miller, J. N. Eckstein, I. Bozovic, and Z.-X. Shen, Science **282**, 2067 (1998).
[22] M. Ogata and H. Fukuyama, Rep. Prog. Phys. **71**, 036501 (2008).
[23] T. Tohyama and S. Maekawa, Supercond. Sci. Technol. **13**, R17 (2000).
[24] J.-Y. P. Delannoy, M. J. P. Gingras, P. C. W. Holdsworth, and A.-M. S. Tremblay, Phys. Rev. B **79**, 235130 (2009).
[25] H. Eskes and G. A. Sawatzky, Phys. Rev. B **44**, 9656 (1991).
[26] B. O. Wells, Z.-X. Shen, A. Matsuura, D. M. King, M. A. Kastner, M. Greven, and R. J. Birgeneau, Phys. Rev. Lett. **74**, 964 (1995).
[27] C. L. Henley, Phys. Rev. Lett. **62**, 2056 (1989).
[28] P. Chandra, P. Coleman, and A. I. Larkin, Phys. Rev. Lett. **64**, 88 (1990).
[29] C. Weber, L. Capriotti, G. Misguich, F. Becca, M. Elhajal, and F. Mila, Phys. Rev. Lett. **91**, 177202 (2003).
[30] Y. Kamiya, N. Kawashima, and C. D. Batista, Phys. Rev. B **84**, 214429 (2011).
[31] A. T. Bollinger, G. Dubuis, J. Yoon, D. Pavuna, J. Misewich, and I. Božović, Nature (London) **472**, 458 (2011).
[32] Y. Kohsaka, M. Azuma, I. Yamada, T. Sasagawa, T. Hanaguri, M. Takano, and H. Takagi, J. Am. Chem. Soc. **124**, 12 275 (2002).
[33] K. M. Shen *et al.*, Phys. Rev. Lett. **93**, 267002 (2004).